

PLASTIC STRENGTH OF MASONRY SHEAR WALLS

H R GANZ, Research Assistant

B THÜRLIMANN, Professor

Institute of Structural Engineering, Swiss Federal Institute of Technology,
Zurich, Switzerland

ABSTRACT The paper presents a summary of a research project carried out at the Swiss Federal Institute of Technology on the behaviour of masonry shear walls. A general failure criterion for masonry under biaxial compressive stresses is presented. Using the theory of plasticity and this failure criterion, lower bounds of the ultimate shear load of masonry walls loaded by normal force and shear are calculated. Thus, a normal force-shear interaction curve is obtained. The extension to the case with an additional bending moment is indicated. Finally, the theoretical results are compared with full scale tests. Twelve panel tests on the failure criterion of masonry and further seven tests on shear walls have been performed.

1. INTRODUCTION

Current design practice for masonry shear walls is usually based on semi-empirical methods. The specified nominal shear stresses are calibrated with experimental results.

Recent design procedures try to consider the physical behaviour of structures more realistically. For steel and concrete structures the theory of plasticity has been used successfully to determine the ultimate load. It is therefore tempting to apply this theory also to masonry.

A research project on the behaviour of masonry shear walls has been carried out. A new design method, based on limit states, is being developed. The paper presents a brief summary of these investigations.

2. LOWER BOUND THEOREM OF THE THEORY OF PLASTICITY

The ultimate load of masonry shear walls can be calculated using the lower and the upper bound theorems of the theory of plasticity. For the design of structures, the lower bound theorem is preferred because the calculated load never exceeds the ultimate load. Furthermore, a statically admissible stress distribution in the whole structure is known such that a proper detailing of all components is possible. Hence, the theoretical derivations in this paper are restricted to the use of the lower bound theorem. It may be formulated as follows:

"A load F_s , calculated from a statically admissible stress field that nowhere violates the failure criterion of the material, is a lower bound of the ultimate load F_u "

$$F_s \leq F_u \quad (1)$$

A stress field is statically admissible if it satisfies equilibrium and the statical boundary conditions.

For the application of the lower bound theorem a failure criterion for masonry and statically admissible stress fields are needed. The practical application of the theory of plasticity requires a sufficient amount of ductility of the material. Whether this ductility is available or not can only be determined by experiments.

3. FAILURE CRITERION FOR MASONRY

In this section, only a brief summary of the complete derivation [1], [2] of the failure criterion for masonry can be given. Masonry is composed of bricks and mortar joints. Therefore, a failure criterion for masonry should consider failure in both components.

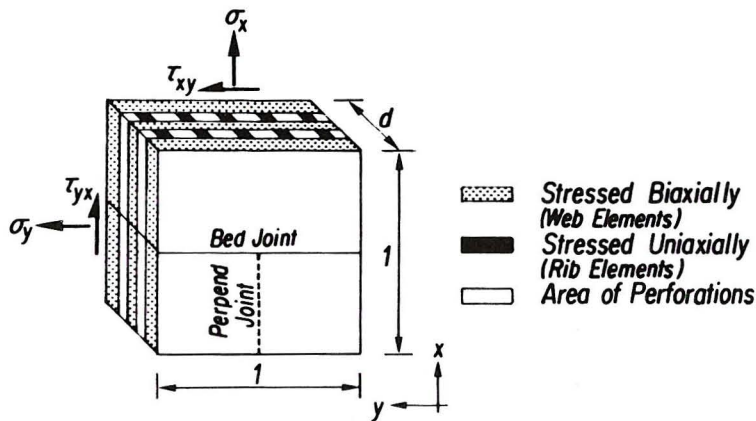


Fig 1 Masonry Element

Usually, bricks are perforated perpendicular to the bed joints. Thus, the net cross sectional area perpendicular to the x-axis is greater than the net cross sectional area perpendicular to the y-axis (Fig. 1).

The total net cross sectional area can be divided into biaxially stressed elements (web elements) and into uniaxially stressed elements (rib elements). Summing up the resistance of the uniaxially and the biaxially stressed isotropic elements,

an anisotropic compressive strength is obtained. The joints reduce this strength to the masonry strengths f_{mx} and f_{my} .

The maximum shear stress is limited by the strength of the biaxially stressed elements (Fig. 2). For the shear resistance of the bed joints, a COULOMB failure criterion with a zero-tension cut-off is assumed. The perpend joints do not enter the failure criterion in case of biaxial compression.

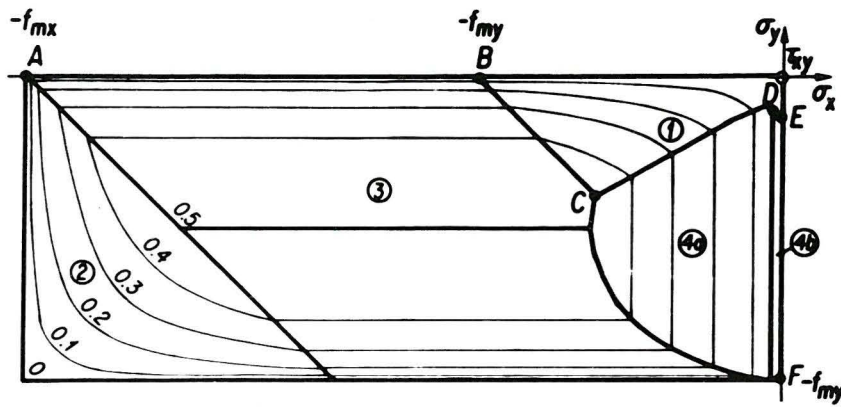
Neglecting any tensile strength, the failure criterion for masonry is given by:

- ① $\tau_{xy}^2 - \sigma_x \cdot \sigma_y = 0$ (no tension in bricks)
- ② $\tau_{xy}^2 - (\sigma_x + f_{mx}) \cdot (\sigma_y + f_{my}) = 0$ (resistance of web and rib elements)
- ③ $\tau_{xy}^2 + \sigma_y \cdot (\sigma_y + f_{my}) = 0$ (resistance of web elements) (2)
- ④a $\tau_{xy}^2 - (c - \sigma_x \cdot \tan \varphi)^2 = 0$ (sliding of bed joints)
- ④b $\tau_{xy}^2 + \sigma_x \cdot [\sigma_x + 2 \cdot c \cdot \tan(\frac{\pi}{4} + \frac{\varphi}{2})] = 0$ (no tension in bed joints)

Figure 2 shows a three-dimensional representation of the failure criterion for a typical set of parameters. Each of the five different domains of the failure criterion represents a specific failure mode (see equation (2)). The failure criterion includes four parameters:

- f_{mx} : masonry compressive strength in x-direction
- f_{my} : masonry compressive strength in y-direction
- c : cohesion of bed joint
- φ : angle of friction of bed joint

In the case of solid bricks with equal masonry compressive strength $f_{my} = f_{mx}$, for instance, the cylindrical portion ③ vanishes.



Contour Spacing: $0.1 f_{my}$ Parameter Set :

$f_{my} / f_{mx} = 0.4$

$c / f_{my} = 0.033$

$\tan \varphi = 0.75$

Fig 2 Failure Criterion for Masonry

In an analogous manner, failure criteria for masonry with tensile strength [1] or reinforced masonry [2] have been developed.

4. STRESS FIELDS

4.1 Parallel Compression Field

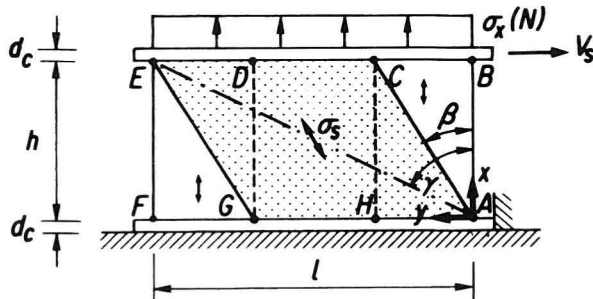


Fig 3 Parallel Compression Field

field is only governing if the stress state in the inclined field (superposition ACH)

$$\begin{aligned}\sigma_x &= \sigma_s \cdot \cos^2 \beta + \sigma_x(N) \\ \sigma_y &= \sigma_s \cdot \sin^2 \beta \\ \tau_{xy} &= \sigma_s \cdot \sin \beta \cdot \cos \beta\end{aligned}\tag{3}$$

reaches the failure surface in the domains (2) and (3) of the failure criterion. Inserting Eq. (3) in the domains (2) and (3) of the failure criterion, Eq. (2), the stress σ_s can be determined

$$\begin{aligned}\textcircled{2} : \sigma_s &= -f_{my} \cdot \frac{f_{mx} + \sigma_x(N)}{(f_{mx} + \sigma_x(N)) \cdot \sin^2 \beta + f_{my} \cdot \cos^2 \beta} > -f_{my} \\ \textcircled{3} : \sigma_s &= -f_{my}\end{aligned}\tag{4}$$

The formulation of the equilibrium in a horizontal section gives the lower bound of the ultimate shear load

$$V_s(\beta) = -\tau_{xy} \cdot d \cdot (1 - h \cdot \tan\beta) = -\sigma_s \cdot \sin\beta \cdot \cos\beta \cdot d \cdot l \cdot (1 - \frac{h}{l} \cdot \tan\beta) \quad (5)$$

where σ_s can be replaced by Eq. (4). The best lower bound can be found by numerical variation of the inclination β . If domain ③ is governing, the best lower bound is

$$V_s = \frac{1}{2} \cdot f_{my} \cdot l \cdot d \cdot \tan\left(\frac{\gamma}{2}\right) \quad (6)$$

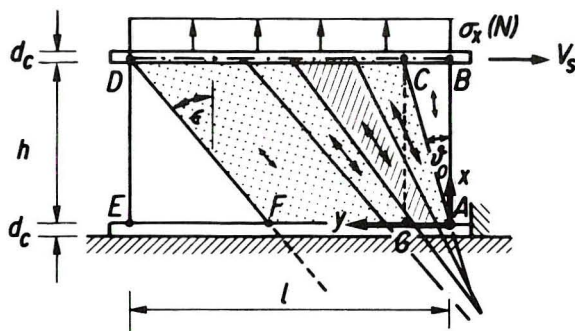
$$\tan\gamma = l/h$$

Thus, the nominal shear stress

$$\tau_{nom} = \frac{V_s}{l \cdot d} = \frac{1}{2} \cdot f_{my} \cdot \tan\left(\frac{\gamma}{2}\right) \quad (7)$$

is a function of the masonry compressive strength f_{my} and of the aspect ratio l/h .

4.2 Non-Centred Fan



This statically admissible field (Fig. 4) is formed by the superposition of two uniaxial stress fields. A vertical parallel field (ABCG) takes part of the normal force. The compression fan (ACDF) carries the total shear V_s and the remainder of the normal force. Therefore, all stress components in the triangle DEF vanish. The inclination ϑ_0 is the parameter of this stress field.

Fig 4 Non-Centred Fan

(Fig.4, edge A to E), the stresses are maximal. They can be calculated for an infinitesimal fan segment (Fig. 5).

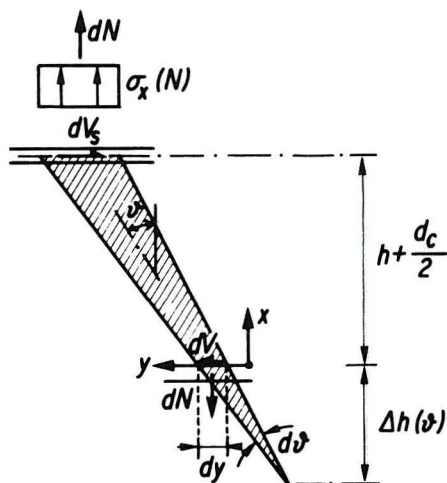


Fig 5 Fan Segment

The stress state in the compression fan is variable. At the boundary $x = 0$

$$x = 0:$$

$$\begin{aligned} \sigma_x(\vartheta) &= \sigma_x(N) \cdot \frac{h + d_c/2}{\Delta h(\vartheta)} \\ \sigma_y(\vartheta) &= \sigma_x(N) \cdot \tan^2\vartheta \cdot \frac{h + d_c/2}{\Delta h(\vartheta)} \\ \tau_{xy}(\vartheta) &= \sigma_x(N) \cdot \tan\vartheta \cdot \frac{h + d_c/2}{\Delta h(\vartheta)} \end{aligned} \quad (8)$$

These stresses must not violate the failure criterion. It can be shown that the non-centred fan is only governing if the stress state at the boundary $x = 0$ reaches the ultimate stresses in the domains ③ and ④ of the failure criterion.

Inserting Eq. (8) in the equations for these domains, the centre of the fan segment can be determined.

$$\Delta h(\vartheta) = \frac{-\sigma_x(N) \cdot (h + d_c/2)}{f_m(\vartheta) \cdot \cos^2 \vartheta + \sigma_x(N)} \quad (9)$$

Considering the range of values of ϑ , the masonry compressive strength $f_m(\vartheta)$ is given by the minimum of the following expressions:

$$\begin{aligned} \textcircled{3} : f_m(\vartheta) &= f_{my} & , 0 < \vartheta \leq \frac{\pi}{2} \\ \textcircled{4a} : f_m(\vartheta) &= \frac{c}{\sin \vartheta \cdot \cos \vartheta - \cos^2 \vartheta \cdot \tan \varphi} \leq f_{my} & , \varphi < \vartheta \leq \frac{\pi}{4} + \frac{\varphi}{2} \\ \textcircled{4b} : f_m(\vartheta) &= 2 \cdot c \cdot \tan\left(\frac{\pi}{4} + \frac{\varphi}{2}\right) & , \frac{\pi}{4} + \frac{\varphi}{2} \leq \vartheta < \frac{\pi}{2} \end{aligned} \quad (10)$$

With Eqs. (9) and (10), all stress components, Eq. (8), are known. The equation of equilibrium, formulated for a fan segment in the section $x = 0$ gives

$$dV(\vartheta) = -\tau_{xy}(\vartheta) \cdot d \cdot d_y = -\sigma_x(N) \cdot f_m(\vartheta) \cdot d \cdot \frac{h + d_c/2}{f_m(\vartheta) \cdot \cos^2 \vartheta + \sigma_x(N)} \cdot \tan \vartheta \cdot d\vartheta \quad (11)$$

where $f_m(\vartheta)$ can be replaced by Eq. (10). Numerical integration of Eq. (11) establishes the lower bound V_s of the ultimate shear load V_u .

$$V_s(\vartheta_0) = \int_{\vartheta_0}^{\varepsilon} dV \quad (12)$$

The best lower bound can be found by numerical variation of the lower limit ϑ_0 of the integral. The last ray of the non-centred fan has to pass through point D in Fig. 4. The upper limit ε of the integral in Eq. (12) follows from this restriction.

The lower bound V_s is a function of the stress due to normal force $\sigma_x(N)$, the failure criterion for masonry and the aspect ratio l/h .

5. INTERACTION CURVES

By evaluating the stress fields "non-centred fan" and "parallel compression field" as a function of the normal force, lower bounds of the normal force-shear interaction curve are obtained. Figure 6 shows lower bounds of the interaction curves for a typical set of material parameters and two aspect ratios l/h .

Between the origin and point A, the non-centred fan is governing. Upper bound solutions can be found, where the differences to the presented interaction curves are less than 10 % [1]. Along the remaining parts of the curves, the parallel compression field is governing. Between the points A and B, domain $\textcircled{3}$ of the failure criterion is controlling. This part of the curves represents the exact ultimate shear load. Between the points B and C, masonry fails in domain $\textcircled{2}$. The indicated solution gives relatively low shear loads. Better lower bounds are obtained if parallel stress fields with variable stress intensity σ_s are calculated (Fig. 6) [1].

The interaction curves are only functions of the material parameters (f_{mx} , f_{my} , c , φ) and the wall aspect ratio (l/h). The plateau AB in Fig. 6 vanishes for ratios $f_{my}/f_{mx} \gtrsim 0.6$.

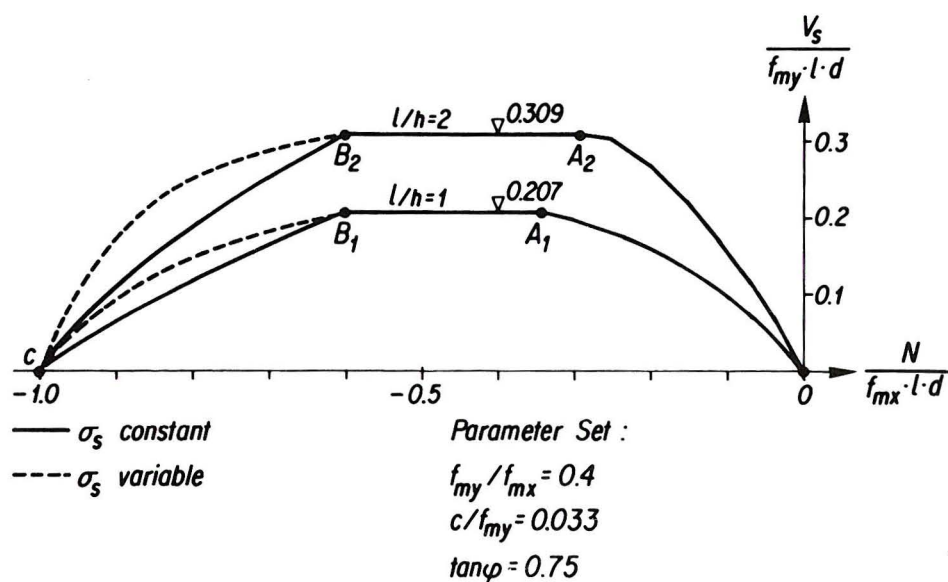


Fig 6 Interaction Curves Normal Force-Shear

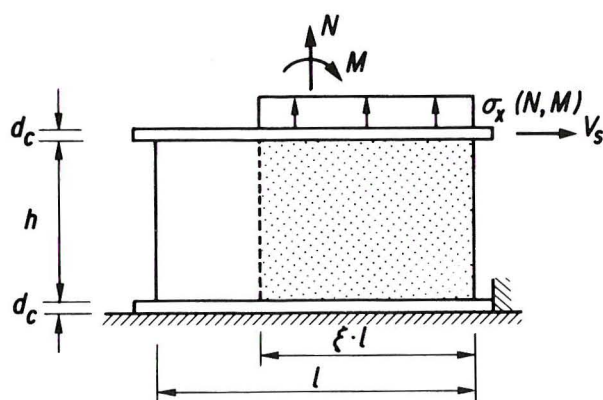


Fig 7 Influence of Bending Moment

$$\xi = 1 - 2 \cdot \frac{M}{N \cdot l} \quad (13)$$

$$\sigma_x(N, M) = \frac{N}{\xi \cdot l \cdot d} \geq -f_{mx}$$

A detailed presentation of these and further more refined stress fields is being prepared [1].

6. COMPARISON WITH TEST RESULTS

6.1 Panel Tests for Checking the Failure Criterion

Twelve panel tests to spot check the theoretically derived failure criterion for masonry have been carried out [3], [4]. The specimens were 1200 mm square and 150 mm thick. Bricks (300 x 190 x 150 mm) with a compressive strength of 31 N/mm² (based on gross area, area of perforations 46%) and a cement mortar with a compressive strength of 28.5 N/mm² were used. The special type of perp joint is shown in Fig. 8. The specimens were loaded biaxially, the principle stresses having various inclinations to the bed joints. Biaxial tension-compression as well as biaxial compression tests (Fig. 9) were performed.

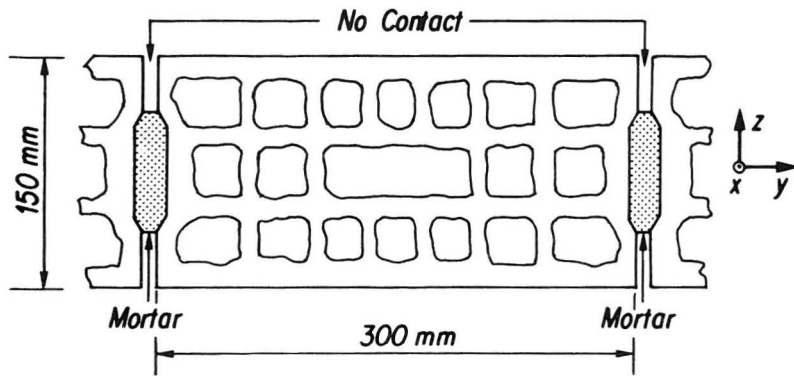


Fig 8 Brick and Perpend Joint

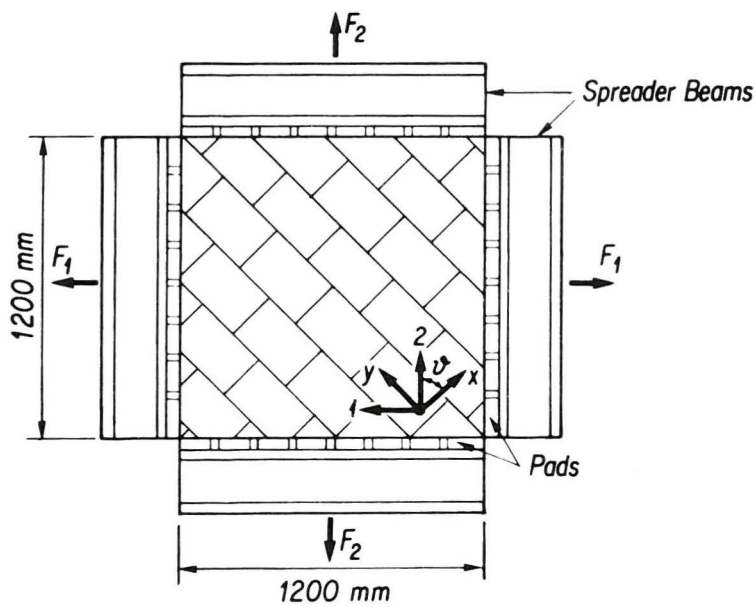


Fig 9 Test Set-up for Biaxial Compression

Test	σ_1 / σ_2	ψ [Degree]	Experiment			Theory			Theory Experiment
			σ_x	σ_y [N/mm ²]	τ_{xy}	σ_x	σ_y [N/mm ²]	τ_{xy}	
K 3	0	0.0	-7.63	0.00	0.00	-7.60	0.00	0.00	1.00
K 4	0	90.0	0.00	-1.83	0.00	0.00	-2.70	0.00	1.48
K 6	0	45.0	-0.32	-0.32	0.32	-0.32	-0.32	0.32	1.00
K 7	0	22.5	-2.25	-0.39	0.93	-2.30	-0.40	0.95	1.02
K 8	0	67.5	-0.04	-0.22	0.09	-0.04	-0.22	0.09	1.00
K10	0.328	0.0	-6.44	-2.11	0.00	-7.60	-2.49	0.00	1.18
K11	0.306	22.5	-4.49	-2.04	1.23	-4.73	-1.98	1.19	0.97
K12	0.304	45.0	-2.03	-2.03	1.08	-2.10	-2.10	1.12	1.03

Parameter Set:
 $f_{mx} = 7.6 \text{ N/mm}^2$
 $f_{my} = 2.7 \text{ N/mm}^2$
 $c = 0.06 \text{ N/mm}^2$
 $\tan \phi = 0.81$

Table 1 Panel Tests on the Failure Criterion

Table 1 gives a summary of the test parameters as well as the experimental and the theoretical ultimate stresses. The material parameters are also indicated. Except for specimen K 4, fair agreement between theory and experiment is obtained.

6.2 Tests on Shear Walls

Seven full scale tests on shear walls have been carried out [4], [5]. The lower and upper edges of the walls were framed by a reinforced concrete slab (Fig.10). The flange width of the specimens W 4 and W 5 was 900 mm. Bricks with a compressive strength of 37.4 N/mm^2 (based on gross area, area of perforations 46%) and a cement mortar with a compressive strength of 28.5 N/mm^2 were used.

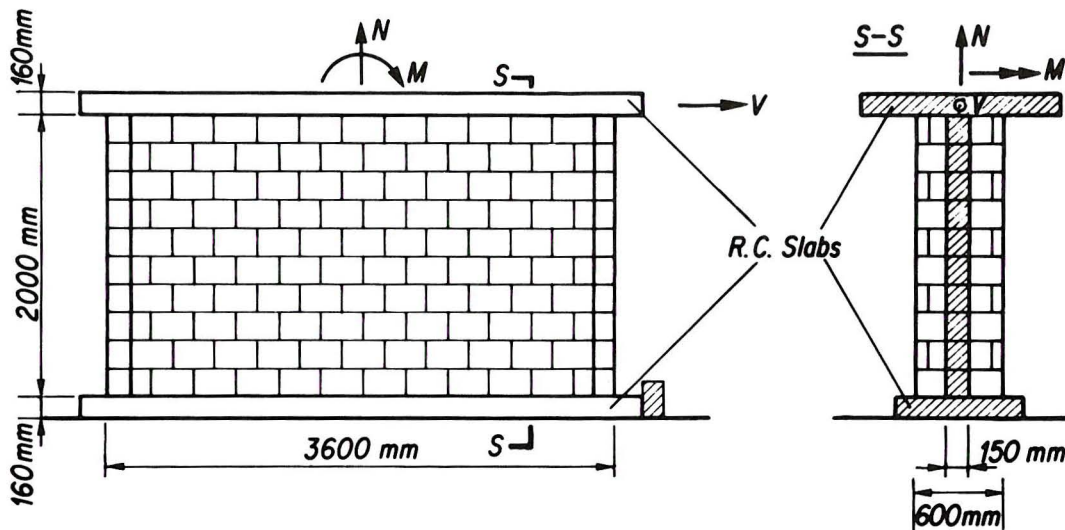


Fig 10 Test Set-up for Shear Walls

The walls were loaded by constant normal force and bending moment. The shear force was then applied through the upper slab and increased up to the failure of the wall. Table 2 gives a summary of the test programme as well as the experimental and theoretical ultimate shear loads. The material parameters are also indicated.

Test	N [kN]	M [mkN]	Bed Joint Reinforcement [mm ² /m]	Loading History	Experiment V_u [kN]	Theory V_s [kN]	$\frac{V_s}{V_u}$
W1	- 415	0	—	static	260	251	0.97
W2	-1287	0	—	static	454	477	1.05
W3	- 415	0	196.4 ¹⁾	static	273	251	0.92
W4	- 423	355.3	—	static	187	125	0.67
W5 ²⁾	- 424	729.3	196.4 ¹⁾	static	365	288	0.79
W6	- 418	0	—	cyclic	247 ^{3)/} 231 ⁴⁾	251/-	1.02
W7	-1290	0	—	cyclic	491 ^{3)/} 438 ⁴⁾	477/-	0.97

1) Yield Stress $f_y = 506 \text{ N/mm}^2$

2) Prestressed Vertically : $P_0 = - 310 \text{ kN}$

$M(P_0) = - 471.2 \text{ mkN}$

3) 1. Cycle

4) 10. Cycle

Parameter Set :

$f_{mx} = 8.25 \text{ N/mm}^2$

$f_{my} = 3.0 \text{ N/mm}^2$

$c = 0.06 \text{ N/mm}^2$

$\tan \varphi = 0.81$

Table 2 Shear Wall Tests

For tests without bending moment, fair agreement between theory and experiment is obtained. In the tests W 4 and W 5, the simple approach of a rectangular stress distribution (Fig. 7) and rectangular cross-section underestimates the ultimate shear load considerably. Nevertheless, more refined stress fields give ratios V_s/V_u between 0.8 to 0.95.

The close prediction of the ultimate loads proves that masonry shear walls exhibit a sufficient amount of ductility for a successful application of the theory of plasticity.

7. CONCLUSIONS

A general anisotropic failure criterion for masonry under biaxial compressive stresses has been presented. It includes four independent material parameters to be determined by experiment. Five different domains are distinguished each one representing a specific failure mode. The failure criterion is applicable to different brick-mortar combinations. An extended failure criterion for reinforced masonry has been given elsewhere [2].

Two statically admissible stress fields for shear walls restrained by reinforced concrete slabs are presented. From these stress fields, lower bounds of the ultimate shear load of walls loaded by normal force and shear are obtained. The comparison with test results proves that masonry shear walls show a sufficient amount of ductility to justify the application of the theory of plasticity. Possible extensions to the case with an additional bending moment are indicated. In an analogous manner, also transverse bending moments can be taken into consideration. Using appropriate stress fields, the influence of openings in the wall can easily be considered.

ACKNOWLEDGEMENT

This research project is financially supported by the Swiss Association of Brick and Tile Manufacturers.

REFERENCES

- [1] GANZ H.R. "Mauerwerksscheiben unter Normalkraft, Schub und Biegemoment" (Masonry Walls Loaded by Normal Force, Shear and Bending Moment). Institute of Structural Engineering, ETH Zürich (Thesis, in preparation).
- [2] THÜRLIMANN B., GANZ H.R. "Bruchbedingung für zweiachsig beanspruchtes Mauerwerk" (Failure Criterion for Biaxially Loaded Masonry). Institute of Structural Engineering, ETH Zürich, Report Nr. 143, 1984 (in German). Editor Birkhäuser Basel, Stuttgart and Boston.
- [3] GANZ H.R., THÜRLIMANN B. "Versuche über die Festigkeit von zweiachsig beanspruchtem Mauerwerk" (Experimental Strength of Biaxially Loaded Masonry). Institute of Structural Engineering, ETH Zürich, Report Nr. 7502-3, 1982. Editor Birkhäuser Basel, Stuttgart and Boston.
- [4] GANZ H.R., THÜRLIMANN B. "Strength of Brick Walls under Normal Force and Shear". The 8th International Symposium on Loadbearing Brickwork, London, November 1983.
- [5] GANZ H.R., THÜRLIMANN B. "Versuche an Mauerwerksscheiben unter Normalkraft und Querkraft" (Tests on Masonry Walls under Normal Force and Shear). Institute of Structural Engineering, ETH Zürich, Report Nr. 7502-4, 1984. Editor Birkhäuser Basel, Stuttgart and Boston.

NOTATION

x	axis perpendicular to bed joint
y	axis parallel to bed joint
σ_x	normal stress perpendicular to bed joint
σ_y	normal stress parallel to bed joint
τ_{xy}	shear stress in the direction of joints
$\sigma_x(N)$	normal stress due to normal force
f_{mx}	masonry uniaxial compressive strength perpendicular to bed joint
f_{my}	masonry uniaxial compressive strength parallel to bed joint
c	cohesion in the bed joint
ϕ	angle of friction in the bed joint
N	normal force
V	shear force
M	bending moment
l	length of shear wall
h	height of shear wall
d	thickness of shear wall
d_c	thickness of concrete slab